1997-11

Nonlinear Optimal Control of a Hydraulically Actuated Positioning System

Timothy McLain
Mechanical Engineering Department, Brigham Young University, mclain@byu.edu

Randal W. Beard
Department of Electrical Engineering, Brigham Young University, beard@ee.byu.edu

Original Publication Citation

McLain, T. and Beard, R. Nonlinear Optimal Control of a Hydraulically Actuated Positioning System, Proceedings of the International Mechanical Engineering Congress and Exposition, FPST Division, vol. 4, pp. 163-168, November 1997, Dallas, Texas.

For presentation at the FPST Division, 1997 IMECE.

Nonlinear Optimal Control of a Hydraulically Actuated Positioning System

Timothy W. McLain
Department of Mechanical Engineering
Brigham Young University
Provo, UT 84602

Randal W. Beard
Department of Electrical Engineering
Brigham Young University
Provo, UT 84602

Abstract

In this paper, the nonlinear optimal control problem is formulated for the position control of an electrohydraulic servo system. The optimal control is given by the solution to the Hamilton-Jacobi-Bellman equation, which in this case cannot be solved explicitly. An alternative method, based upon successive Galerkin approximation, is used to obtain an approximate optimal solution. Preliminary simulation results, demonstrating the application of this approach to the position control of a hydraulically actuated device, are presented.

1 Introduction

In the synthesis of controllers for fluid-power actuation systems, a common approach is to linearize the nonlinear dynamics of the system and then to design the controller using a linear control design methodology [1, 2]. In this paper, a new approach is taken wherein a nonlinear feedback controller is synthesized based upon the full nonlinear dynamics of the system. This approach involves the formulation of the nonlinear optimal control problem, which is expressed as a nonlinear partial differential equation, and its approximate computational solution by successive applications of a Galerkin-type method.

Though the off-line computations are quite intense, this strategy eliminates the need for linearization, whether explicit or through feedback, while providing a control law that compensates for the nonlinear dynamics of the system in an optimal way. While this successive Galerkin approximation (SGA) technique has been applied to a variety of problems [3], this paper represents initial efforts to apply the SGA methodology to a system representative of an industrial "real-world" application.

2 Control Approach

Given a system modeled by the nonlinear state equations

$$\dot{x} = f(x) + g(x)u(x) \tag{1}$$

and the performance index

$$V(x) = \int_t^\infty \left(l(x) + \|u(x)\|_R^2 \right) dt, \tag{2}$$

[1] the "optimal" control which minimizes the performance index is given by

$$u^*(x) = -\frac{1}{2} R^{-1} g^T(x) \frac{\partial V^*}{\partial x} \tag{3}$$

where $V^*(x)$ is a positive definite function that satisfies the Hamilton-Jacobi-Bellman (HJB) equation:

$$\frac{\partial V^{*T}}{\partial x} f(x) + l(x) - \frac{1}{4} \frac{\partial V^{*T}}{\partial x} g(x) R^{-1} g^T(x) \frac{\partial V^*}{\partial x} = 0. \tag{4}$$

Obtaining a closed-form solution of Equation 4 for systems of the complexity of the hydraulic actuation system under consideration is impossible. The approach for solving the HJB equation presented here is to begin with a known control, $u^{(0)}$ (*e.g.* PD control), that is stabilizing over a bounded domain of the state space Ω and to numerically compute successive approximations to the optimal control given by Equation 3.

Consider the performance index of Equation 2 with the initial feedback control law $u^{(0)}(x)$:

$$V^{(0)}(x) = \int_t^\infty \left(l(x) + \left\| u^{(0)}(x) \right\|_R^2 \right) dt. \tag{5}$$

Taking the derivative of both sides of Equation 5 with respect to time gives:

$$\frac{\partial V^{(0)T}}{\partial x} \dot{x} = \left(l + \left\| u^{(0)} \right\|_R^2 \right) \Big|_{t=0}^{\infty}.$$

[1] Though $l(x)$ can be any positive definite function of x, it is commonly chosen to be $\|x\|_Q^2 = x^T Q x$.

Since $u^{(0)}$ is asymptotically stabilizing, $(x, u^{(0)}) \to 0$ as $t \to \infty$, which results in the partial differential equation

$$\frac{\partial V^{(0)T}}{\partial x}\left[f + gu^{(0)}\right] + l + \left\|u^{(0)}\right\|_R^2 = 0. \tag{6}$$

Equations 5 and 6 show that $V^{(0)}$ is a Lyapunov function for the control $u^{(0)}$. Given $V^{(0)}$, the stability and robustness of $u^{(0)}$ can be improved by choosing a new control $u^{(1)}$ such that

$$\begin{aligned} u^{(1)} &= \arg\min_u \left[\frac{\partial V^{(0)T}}{\partial x}(f + gu) + l + \|u\|_R^2\right] \\ &= -\frac{1}{2}R^{-1}g^T\frac{\partial V^{(0)}}{\partial x}. \end{aligned} \tag{7}$$

Note that along state trajectories of the system under the control of $u^{(1)}$,

$$\begin{aligned} \dot{V}^{(0)} &= \frac{\partial V^{(0)T}}{\partial x}(f + gu^{(1)}) \\ &= -l - \|u^{(1)}\|_R^2 \\ &\leq -l - \|u^{(0)}\|_R^2 \\ &\leq 0, \end{aligned}$$

and thus $u^{(1)}$ as found from Equation 7 represents an improvement over $u^{(0)}$.

Equations 6 and 7 can be generalized to form the basis for an iterative solution process where

$$\frac{\partial V^{(i)T}}{\partial x}\left[f + gu^{(i)}\right] + l + \left\|u^{(i)}\right\|_R^2 = 0 \tag{8}$$

$$u^{(i+1)} = -\frac{1}{2}R^{-1}g^T\frac{\partial V^{(i)}}{\partial x}. \tag{9}$$

Equation 8 is known as the Generalized Hamilton-Jacobi-Bellman (GHJB) equation [3]. By starting with a known $u^{(0)}$ and iteratively solving Equations 8 and 9, successive values for $V^{(i)}$ and $u^{(i)}$ are found which have been shown to converge monotonically to the optimal values V^* and u^* given by Equations 4 and 3 respectively [4, 5].

The problem of formulating the near-optimal control is simplified to solving the GHJB equation, which is a linear, first-order partial differential equation. While Equation 8 cannot, in general, be solved analytically, it is more amenable to numerical solution than the HJB equation.

2.1 Numerical Solution of the GHJB

To solve the GHJB Equation, a computational Galerkin method is employed [6]. It is first assumed that $V^{(i)}$ can be written as an infinite series of known basis functions $\phi_j(x)$ that are continuous and defined everywhere on Ω, *i.e.*,

$$V^{(i)} = \sum_{j=1}^{\infty} c_j^{(i)}\phi_j^{(i)}(x).$$

An approximation to the assumed solution $V^{(i)}$ having the desired degree of accuracy can be formed by considering the first N terms of the infinite series:

$$V_N^{(i)} = \sum_{j=1}^{N} c_j^{(i)}\phi_j^{(i)}(x). \tag{10}$$

By substituting Equation 10 into Equation 8, an expression for the resulting error $e^{(i)}$ is obtained:

$$e^{(i)}(x) = \left(\sum_{j=1}^{N} c_j^{(i)}\frac{\partial \phi_j^T}{\partial x}\right)\left[f + gu^{(i)}\right] + l + \left\|u^{(i)}\right\|_R^2. \tag{11}$$

Defining the inner product of two functions f and g in the following manner,

$$\langle f(x), g(x)\rangle_\Omega \triangleq \int_\Omega f(x)g(x)dx$$

the error can be projected onto the N basis functions $\phi_1, \phi_2, \ldots, \phi_N$ on a closed and bounded set Ω and set to zero to obtain N linear equations in N unknowns $(c_1^{(i)}, c_2^{(i)}, \ldots, c_N^{(i)})$:

$$\left\langle e^{(i)}(x), \phi_j(x)\right\rangle_\Omega = 0, \quad j = 1 \ldots N. \tag{12}$$

This system of equations can be solved to find $c^{(i)} = [c_1^{(i)}\ c_2^{(i)}\ \cdots\ c_N^{(i)}]^T$. With these coefficients identified, the functional expression for the control associated with the $(i+1)^{th}$ iteration can be calculated.

2.2 SGA Feedback Synthesis Algorithm

Although fairly simple conceptually, the computation of Equation 12 is quite complex to carry out. The computation of the coefficients which form the basis of the near-optimal control law are performed according to the algorithm below.

Input: $f, g, l, R, \Omega, \{\phi_j\}_1^N, u^{(0)}$.

Compute the matrices: $A_1, A_2, b_1, b_2, \{M_i\}_1^N$ where

$$A_1 = \begin{bmatrix} \left\langle \frac{\partial \phi_1^T}{\partial x} f, \phi_1 \right\rangle_\Omega & \cdots & \left\langle \frac{\partial \phi_N^T}{\partial x} f, \phi_1 \right\rangle_\Omega \\ \vdots & \ddots & \vdots \\ \left\langle \frac{\partial \phi_1^T}{\partial x} f, \phi_N \right\rangle_\Omega & \cdots & \left\langle \frac{\partial \phi_N^T}{\partial x} f, \phi_N \right\rangle_\Omega \end{bmatrix}$$

$$A_2 = \begin{bmatrix} \left\langle \frac{\partial \phi_1^T}{\partial x} g u^{(0)}, \phi_1 \right\rangle_\Omega & \cdots & \left\langle \frac{\partial \phi_N^T}{\partial x} g u^{(0)}, \phi_1 \right\rangle_\Omega \\ \vdots & \ddots & \vdots \\ \left\langle \frac{\partial \phi_1^T}{\partial x} g u^{(0)}, \phi_N \right\rangle_\Omega & \cdots & \left\langle \frac{\partial \phi_N^T}{\partial x} g u^{(0)}, \phi_N \right\rangle_\Omega \end{bmatrix}$$

$$b_1 = -\begin{bmatrix} \langle l, \phi_1 \rangle_\Omega \\ \vdots \\ \langle l, \phi_N \rangle_\Omega \end{bmatrix}$$

$$b_2 = -\begin{bmatrix} \left\langle \left\| u^{(0)} \right\|_R^2, \phi_1 \right\rangle_\Omega \\ \vdots \\ \left\langle \left\| u^{(0)} \right\|_R^2, \phi_N \right\rangle_\Omega \end{bmatrix}$$

$$\{M_i\}_1^N = \begin{bmatrix} m_i(1,1) & \dots & m_i(1,N) \\ \vdots & \ddots & \vdots \\ m_i(N,1) & \dots & m_i(N,N) \end{bmatrix}$$

$$m_i(j,k) = \left\langle \frac{\partial \phi_k^T}{\partial x} g R^{-1} g^T \frac{\partial \phi_i}{\partial x}, \phi_j \right\rangle_\Omega$$

Initial step:

$$\begin{aligned} A &= A_1 + A_2 \\ b &= b_1 + b_2 \\ c^{(0)} &= A^{-1} b \\ i &= 1 \end{aligned}$$

Iteration step:

$$\begin{aligned} A_2 &= -\tfrac{1}{2} \textstyle\sum_{j=1}^N c_j^{(i-1)} M_j \\ b_2 &= -\tfrac{1}{4} \begin{bmatrix} c^{(i-1)T} M_1 c^{(i-1)} \\ c^{(i-1)T} M_2 c^{(i-1)} \\ \vdots \\ c^{(i-1)T} M_N c^{(i-1)} \end{bmatrix} \\ A &= A_1 + A_2 \\ b &= b_1 + b_2 \\ c^{(i)} &= A^{-1} b \\ i &= i + 1 \end{aligned}$$

Output:

$$u_N^{(i)} = -\frac{1}{2} R^{-1} g^T \left(\sum_{j=1}^N c_j^{(i)} \frac{\partial \phi_j}{\partial x} \right). \qquad (13)$$

3 Hydraulic Actuation System Model

The hydraulic actuation system modeled is shown in Figure 1 below. It consists of a four-way servovalve driving a linear piston connected to an inertial load. The model developed here is similar in many respects to previously developed models [1, 7]. For simplicity, the electromechanical portion of the servovalve (not depicted in Figure 1) is modeled as a first-order system with the current to the valve, i_v, as the input. The orifice characteristics are patterned after those of a Moog Model 31 servovalve.

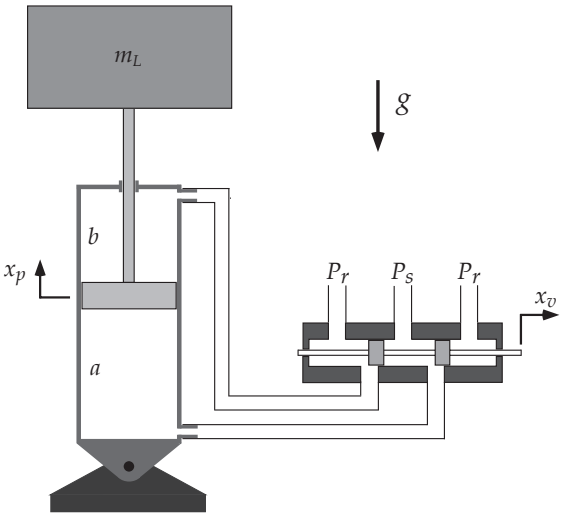

Figure 1: System Schematic Diagram

The state variables for the model are P_a – pressure on the "a" side of the piston, P_b – pressure on the "b" side of the piston, v_p – piston velocity, x_p – piston position, and x_v – the servovalve spool position.

To correctly model the behavior of the valve, two separate operating conditions must be considered: the upstroke where $x_v \geq 0$ and the downstroke where $x_v < 0$. On the upstroke, the orifice between supply pressure and the a side of the piston and the orifice between the b side of the piston and return pressure are opened. Similarly, on the downstroke, orifices between supply pressure and side b and between side a and return are opened.

As might be expected, the equations of motion describing the behavior of the piston pressure states are dependent on whether the valve is in the upstroke or downstroke configuration:

Upstroke: $(x_v \geq 0)$

$$\dot{P}_a = \frac{B}{V_a} \left[C_d h_v x_v \sqrt{\frac{2(P_s - P_a)}{\rho}} - A_a v_p \right] \qquad (14)$$

$$\dot{P}_b = \frac{B}{V_b} \left[-C_d h_v x_v \sqrt{\frac{2(P_b - P_r)}{\rho}} + A_b v_p \right] \qquad (15)$$

Downstroke: $(x_v < 0)$

$$\dot{P}_a = \frac{B}{V_a}\left[C_d h_v x_v \sqrt{\frac{2(P_a - P_r)}{\rho}} - A_a v_p\right] \quad (16)$$

$$\dot{P}_b = \frac{B}{V_b}\left[-C_d h_v x_v \sqrt{\frac{2(P_s - P_b)}{\rho}} + A_b v_p\right] \quad (17)$$

where B is the bulk modulus of the fluid, C_d is the discharge coefficient associated with the valve orifices, h_v is the effective height of the valve orifice, P_a and P_b are cylinder pressures, ρ is fluid density, and A_a and A_b are piston areas. V_a and V_b are the fluid volumes contained by the a and b sides of the cylinder and are dependent on the piston position:

$$V_a = A_a\left(\frac{L}{2} + x_p\right)$$
$$V_b = A_b\left(\frac{L}{2} - x_p\right).$$

Equations of motion for piston velocity, piston position, and valve position are given by

$$\dot{v_p} = \frac{1}{m_L}\left[A_a P_a - A_b P_b - b v_p - F_c \text{sign}(v_p)\right] \quad (18)$$

$$\dot{x_p} = v_p \quad (19)$$

$$\dot{x_v} = -\frac{1}{\tau}x_v + \frac{K_s}{\tau} i_v \quad (20)$$

where friction in the piston is modeled by viscous and coulomb terms, b and F_c, K_s is the valve torque-motor gain, and τ is the torque-motor time constant.

Equations 14 through 20 represent the nonlinear dynamics of the system shown schematically in Figure 1. These equations are of the general form of Equation 1, and from them the functions $f(x)$ and $g(x)$ required for the synthesis of the control can be determined.

4 Control Synthesis and Implementation

With the model described above, the optimal feedback control can be synthesized based on the SGA algorithm. With $f(x)$ and $g(x)$ coming directly from the equations of motion, the cost function on the states $l(x)$, the weighting matrix on the control cost R, the domain of the states Ω, the basis functions $\{\phi_j(x)\}_1^N$, and the initial control law $u^{(0)}$ remain to be determined. For the results presented here, the cost function was chosen to be

$$l(x) = q_1 v_p^2 + q_2 x_p^2 + q_3 (A_a P_a - A_b P_b - m_L g)^2,$$

where q_1, q_2, and q_3 are positive weighting constants. As the goal of the control is to drive $l(x)$ to zero, including the function $A_a P_a - A_b P_b - m_L g$ in the cost function provides a way to regulate the pressure states in a manner consistent with the dynamics of the system without driving them to zero.

Since the system has only a single input (i_v), the weighting matrix on the control (R) is simply a scalar variable. The domain of possible values for the states is governed by the physical limitations of the system:

$$P_r \le P_a \le P_s$$
$$P_r \le P_b \le P_s$$
$$-Q_{max}/A_a \le v_p \le Q_{max}/A_a$$
$$x_{p_{min}} \le x_p \le x_{p_{max}}$$
$$x_{v_{min}} \le x_v \le x_{v_{max}}$$

where Q_{max} is the maximum rated no-load flow through the valve, $x_{p_{min}}$ and $x_{p_{max}}$ are the minimum and maximum displacement of the piston, and $x_{v_{min}}$ and $x_{v_{max}}$ are the minimum and maximum displacement of the valve spool.

An understanding of the dynamic behavior of the system plays an important role in the proper selection of the basis functions $\{\phi_j(x)\}_1^N$. For the control to compensate adequately for the nonlinear dynamics of the system, the basis functions must be able to capture the dominant dynamics of the system. For this problem, the following basis functions were used:

$$\begin{aligned}
\phi_1 &= v_p^2 \\
\phi_2 &= x_p^2 \\
\phi_3 &= x_v^2 \\
\phi_4 &= (A_a P_a - A_b P_b - m_L g)^2 \\
\phi_5 &= v_p x_p \\
\phi_6 &= v_p x_v \\
\phi_7 &= v_p (A_a P_a - A_b P_b - m_L g) \\
\phi_8 &= x_p x_v \\
\phi_9 &= x_p (A_a P_a - A_b P_b - m_L g) \\
\phi_{10} &= x_v (A_a P_a - A_b P_b - m_L g).
\end{aligned}$$

An interesting aspect of these basis functions is that absence of $x_v P_a$ and $x_v P_b$ as basis functions. If these basis functions are included, the control (as calculated from Equation 13) will contain independent P_a and P_b terms which attempt to drive P_a and P_b to zero to the detriment of the control of the other states. In this particular problem, the objective is to regulate the states v_p, x_p, and x_v leaving P_a and P_b to vary as necessary to control the piston as desired. Notice that in steady state, the pressures are related by the pressure function $A_a P_a - A_b P_b - m_L g = 0$. By allowing this pressure function to be a part of the basis functions selected, pressure

Table 1: Weighting Functions and Control Laws

Initial Design
$l = {v_p}^2 + {x_p}^2 + (A_aP_a - A_bP_b - m_Lg)^2$
$R = 1$
$u = -0.302v_p + 1.48x_p - 1098x_v$ $-0.0797(A_aP_a - A_bP_b - m_Lg)$
High-Performance Design
$l = 0.2{v_p}^2 + {x_p}^2 + 2(A_aP_a - A_bP_b - m_Lg)^2$
$R = 1$
$u = 0.253v_p - 3.13x_p - 1033x_v$ $-0.0792(A_aP_a - A_bP_b - m_Lg)$
Moderate-Control Design
$l = 0.2{v_p}^2 + {x_p}^2 + 2(A_aP_a - A_bP_b - m_Lg)^2$
$R = 40$
$u = 0.030v_p - 0.556x_p - 91.0x_v$ $-0.00266(A_aP_a - A_bP_b - m_Lg)$

terms enter into the control in a manner consistent with the control objectives of the system.

Finally, the initial stabilizing control was chosen to be PD control:

$$u^{(0)} = -K_p x_p - K_d v_p.$$

With the input parameters defined, optimal control laws can be synthesized using the SGA algorithm. Simulation results for three different controllers are presented.

5 Results

Using the SGA synthesis algorithm with the inputs as described, three different optimal controllers were designed and implemented. Table 1 shows the weighting functions and the corresponding control laws obtained for each of the three controllers. For the test cases presented here, the operating conditions were such that x_v was always less than zero. Though controllers were synthesized for both upstroke and downstroke conditions, only those developed from the downstroke equations of motion are presented.

For an initial design, the state weighting function and control weight were set to

$$l = {v_p}^2 + {x_p}^2 + (A_aP_a - A_bP_b - m_Lg)^2$$

and

$$R = 1.$$

Figure 2 shows the response of the states to a non-zero initial condition on piston position using this initial control design. It should be noted that valve position tracked the valve current signal very closely (differing by gain K_s) and is an accurate indication of the control effort expended in each case. While the valve position, piston position, and piston velocity are eventually regulated to zero, the system's response is more sluggish than desired.

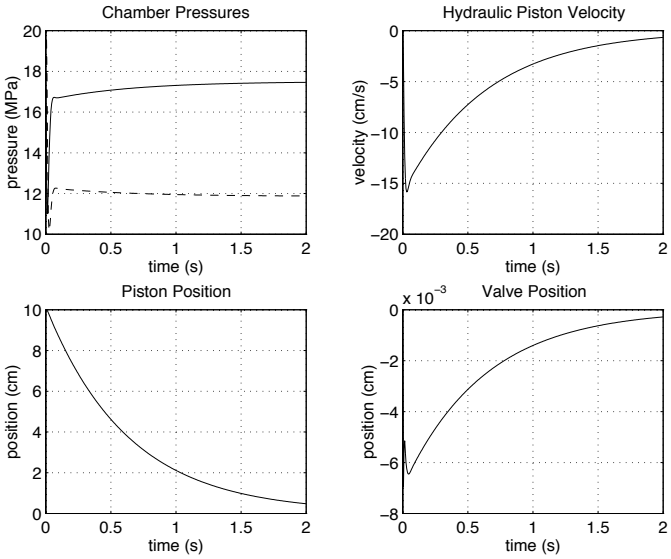

Figure 2: Initial Design

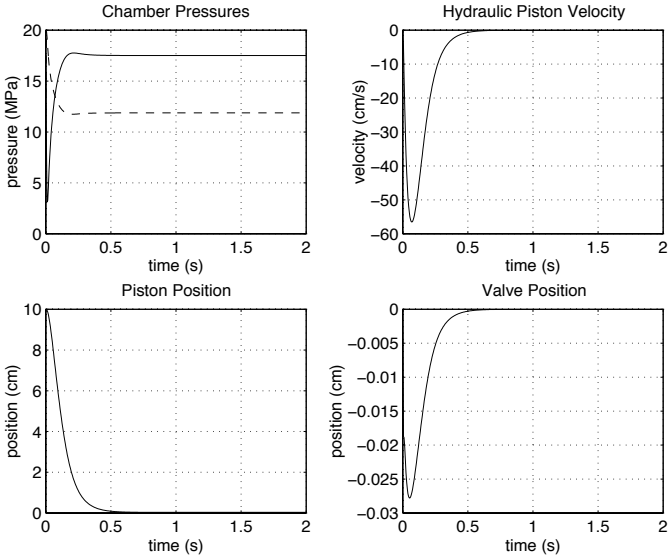

Figure 3: High-Performance Design

As with the design of a linear quadratic regulator, changes in the behavior of this nonlinear actuation system are brought about by changing the state weighting function l and the weight on the control R. As an example of how a designer might decrease the response time of this system, the weighting function was altered by decreasing the weight on the v_p^2 term (from 1 to 0.2) and increasing the weight on the pressure function term (from

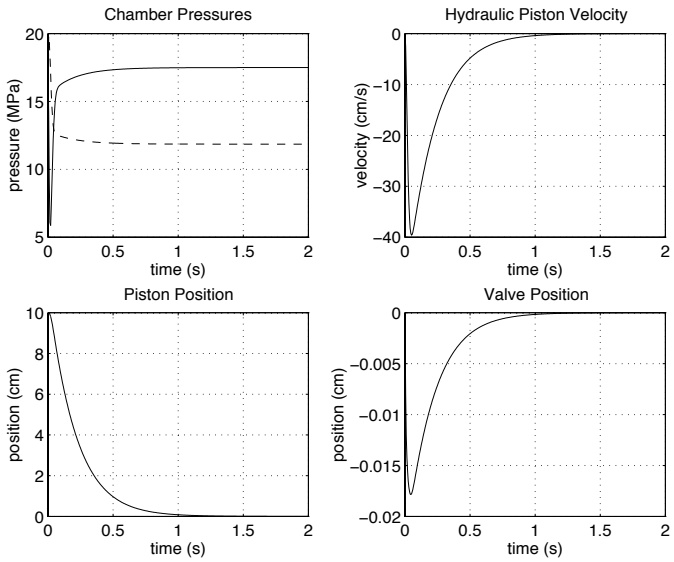

Figure 4: Moderate-Control-Effort Design

1 to 2). These two changes caused the pressure states to be driven to their steady-state values more quickly and allowed the piston velocity to reach higher values initially with the net result being that the piston position was driven to zero in much less time than the case when the initial control was used. In order to bring this improved response about, greater control effort was required.

In the event that the control effort expended for a particular design is too high, more conservative designs can generated by increasing the weight on the control effort. As an example of this, the high-performance design of Figure 3 was moderated by increasing the weight on the control from 1 to 40. The response of this moderate-control-effort design is presented in Figure 4. From this plot, it can be seen that by increasing R, the peak control effort drops significantly. Correspondingly, the time required for the states to settle to their steady-state values increases.

These simulation results demonstrate potential utility of the SGA synthesis approach for developing optimal controllers for nonlinear systems. By tuning the state weighting function and the weight on the control effort appropriately, the behavior of the closed-loop system can be altered to suit the needs of a specific application. Furthermore, by adding more complex basis functions, higher-order nonlinear effects can be compensated for.

6 Conclusions

In this paper, an optimal control strategy based upon successive Galerkin approximation has been applied to the control of a hydraulically actuated positioning system. Using this approach, several optimal controllers were designed taking into account the full nonlinear dynamics of the hydraulic actuation system. Based upon these preliminary results, SGA appears to be a promising approach for control synthesis for systems having nonlinear dynamics.

References

[1] Gholamreza Vossoughi and Max Donath, "Dynamic feedback linearization for electrohydraulically actuated control systems", *ASME Journal of Dynamic Systems, Measurement, and Control*, vol. 117, no. 4, pp. 468–477, 1995.

[2] E. Richard and S. Scavarda, "Comparison between linear and nonlinear control of an electropneumatic servodrive", *ASME Journal of Dynamic Systems, Measurement, and Control*, vol. 118, pp. 245–252, 1996.

[3] Randy Beard, George Saridis, and John Wen, "Improving the performance of stabilizing controls for nonlinear systems", *IEEE Control Systems Magazine*, vol. 16, no. 5, pp. 27–35, 1996.

[4] G.N. Saridis and C.-S.G. Lee, "An approximation theory of optimal control for trainable manipulators", *IEEE Transactions on Systems, Man, and Cybernetics*, vol. SMC-9, pp. 152–159, March 1979.

[5] G.N. Saridis and J. Balaram, "Suboptimal control for nonlinear systems", *Control Theory and Advanced Technology*, vol. 2, pp. 547–562, September 1986.

[6] C.A.J. Fletcher, *Computational Galerkin Methods*, Springer-Verlag, 1984.

[7] T.W. McLain, E.K. Iversen, C.C. Davis, and S.C. Jacobsen, "Development, simulation, and validation of a highly nonlinear hydraulic servosystem model", in *Proceedings of the American Control Conference*, Pittsburgh, PA, 1989, pp. 385–391.